REAL TIME PC IMPLEMENTATION OF POWER QUALITY MONITORING SYSTEM BASED ON MULTIHARMONIC LEAST-SQUARES FITTING

Andrei S. Ardeleanu[1], Pedro M. Ramos[2]

1) *"Gheorghe Asachi" Technical University of Iaşi, Faculty of Electrical Engineering, Energetics and Applied Informatics, 21-23 Professor Dimitrie Mangeron Blvd, 700050, Iaşi, România (a.ardeleanu@ee.tuiasi.ro)*

2) *Instituto de Telecomunicações, Instituto Superior Técnico, Universidade Técnica de Lisboa, Av. Rovisco Pais, 1, 1049-001, Lisbon, Portugal (✉pedro.m.ramos@ist.utl.pt)*

Abstract

In this paper, an algorithm that monitors the power system to detect and classify power quality events in real time is presented. The algorithm is able to detect events caused by waveform distortions and variations of the RMS values of the voltage. Detection of the RMS events is done by comparing the RMS values with certain thresholds, while detection of waveform distortions is made using an algorithm based on multiharmonic leasts-squares fitting.

Keywords: power quality, real time, multiharmonic least-squares fitting.

1. Introduction

Given the fact that increasingly more electrical equipment can cause electromagnetic disturbances and is sensitive to these phenomena, real time power quality monitoring has become, in recent years, an important subject of research. It is estimated that costs of wastage caused by poor power quality in Europe exceed 150bn.€ per year [1] which reinforces the necessity of efficient, cost-effective, real time power quality monitoring.

Power quality can be defined as "the concept of powering and grounding sensitive equipment in a manner that is suitable to the operation of that equipment" [2] or, according to the International Electrotechnical Commission (IEC) as "characteristics of the electricity at a given point on an electrical system, evaluated against a set of reference technical parameters" [3]. Therefore, it can be said that power quality represents a set of parameters regarding the continuity, magnitude and waveform shape of the power delivered to users. Depending on these parameters, power quality events can be classified into two major categories: (i) transients, waveform distortions (ii) short and long duration disturbances (interruptions, sags, swells, undervoltages, overvoltages).

The appearance of these events in power distribution networks can cause harmful effects on power system devices and end users' devices. Malfunctions, increase of losses, decrease of lifetime or even failures are some of the effects that poor power quality can cause on electrical devices.

Power quality monitoring can be performed for different reasons: finding the cause of equipment malfunction and other power quality problems, obtaining statistical information regarding the performance of the equipment, obtaining information about the performance of the power distribution system (quality of service), analyzing system events that led to an interruption or blackout (to help prevent future events) or with permanent power quality

monitoring where no additional measurements are needed for troubleshooting (*i.e.,* recorded data can be used to find the cause of a problem) [4].

In this paper, an algorithm that monitors the power quality and detects the events that are occurring in real time is presented. Real time monitoring can be used to find and solve issues that arise due to poor quality of the power. Electrical devices both create and are sensitive to power quality events and in an environment where they have to work together, some of them can be influenced by the others and might function abnormally. By monitoring the quality of power in real time, connections can be found between the malfunction of a device and a certain event that occurred at that time. Knowing the cause of the problem, solutions can then be implemented to prevent future failures.

Over the past years, several methods for detection and classification of power quality events in a power system were presented [5-17]. The wavelet transform is one of the most often employed signal-processing techniques used for power quality detection algorithms [5-11]. It can successfully detect high frequency events (transients) but in the case of slow disturbances, it performs poorly especially when the voltage variations are not sudden, but gradual. Other solutions include the combined use of wavelets and fuzzy support vector machines [18], wavelets and neural networks [19], pattern recognition [20], time-frequency representations [21] and digital filters [22].

Power quality algorithms can be implemented in devices based on digital signal processors (DSPs) [12-14] or on personal computers (PCs) [15-17]. DSP implementation is rather difficult and time consuming because of the verification process of the algorithm blocks working in real time and computational requirements are more difficult to comply with. Another issue is the limited amount of DSP internal memory available because, although DSPs can use external memory, access to it is much slower than the access to internal memory. In recent years, personal computers have become much faster and cheaper and so they are an important option for implementing algorithms. They are easy to upgrade to fulfill the increasing computational requirements and also have multiple in-built interfaces that make the communication with external devices or data reporting much easier. Data can be saved in different formats and transmitted to remote locations or displayed on an internet page to be separately available. Another important issue is the use of PCs with multiple core processors. Multiple cores can be used to speed up execution of multiple algorithms that can be executed in parallel without significant further development (for example in LabVIEW multiple core execution is embedded and straightforward to use).

The system proposed in this paper, based on a personal computer, monitors the three phases of the power system in order to detect, in real time, power quality events. Data that contains the events is saved on the computer and also on a server as a web page for remote monitoring and dissemination of the project results.

The classification of the events into transients and waveform distortions is done according to their duration and total harmonic distortion (THD) values. The THD values are calculated using the results of a multiharmonic least-squares fitting algorithm [23]. Short and long duration disturbances are detected by monitoring the RMS values of the voltage and comparing it with pre-defined thresholds.

2. Algorithm Description

Voltage measurements are made with three LEM LV 25-P closed-loop Hall effect transducers for the three phases of the power distribution network. The transducer outputs are sampled by a NI USB-9215A data acquisition board at a frequency of 10 kHz connected to a personal computer for processing. Continuous data segments are used by the power quality

algorithm to detect and process the events that are occurring and that may extend throughout multiple data segments.

The block diagram of the proposed algorithm is presented in Fig. 1. The algorithm consists of two parts: one for events caused by changes in RMS values and the other for events caused by transients and distortions in the voltage waveforms.
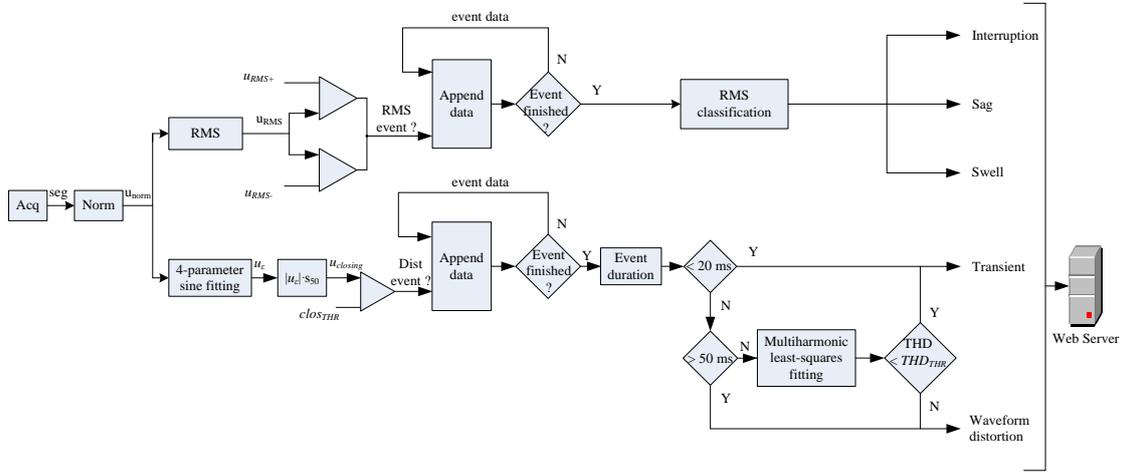

Fig. 1. Block diagram of the implemented algorithm.

2.1. Detection of RMS events

RMS calculation and detection of events (interruptions, sags, swells, undervoltages and overvoltages) is performed according to the IEC 61000-4-30 standard [3]. Normalized values of the voltage signal are used for computing the RMS values obtained at every half of period for one period of data. Zero-crossing points, determined by interpolation, are used to obtain the period of data necessary for RMS calculation. RMS estimation is obtained from

$$u_{RMS} = \sqrt{\frac{\sum_{i=1}^{N_{RMS}} u[i]^2 \times d[i]}{\sum_{i=1}^{N_{RMS}} d[i]}} \ , \tag{1}$$

where N_{RMS} is the number of samples per period, $u[i]$ are the signal samples and $d[i]$ is the sample duration.

Since the RMS values are calculated for periods determined by interpolated zero-crossing points, the values of $d[i]$ will change for the samples in the vicinity of zero crossings. In Fig. 2 a simple example about RMS calculation near a zero-crossing is presented. $u[1]$, $u[2]$, $u[3]$ and $u[4]$ are four samples of the signal, $u[z]$ is the determined zero-crossing sample and $d[z_1]$ and $d[z_2]$ are the durations between the zero-crossing and samples before ($u[2]$) and after ($u[3]$).

The durations for samples $u[1]$ and $u[4]$, which aren't in the vicinity of the zero-crossing, are the sampling period of the signal *i.e.*, $dt = 1/f_s$, where f_s is sampling frequency. For samples $u[2]$ and $u[3]$ the durations are

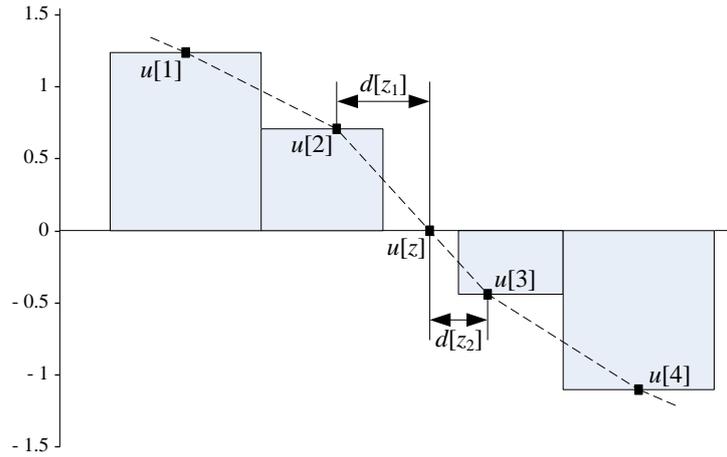$$d[2] = \frac{dt}{2} + \frac{d[z_1]}{2} \text{ and } d[3] = \frac{dt}{2} + \frac{d[z_2]}{2}. \tag{2}$$

Fig. 2. RMS calculation.

If an interruption occurs, zero-crossing points cannot be used to determine the period of data and therefore the signal is assumed to have 50 Hz frequency (the nominal system frequency), for which the period of data is determined.

The estimated RMS values are compared with an upper and lower threshold u_{RMS+} and u_{RMS-}. If the RMS exceeds the upper threshold or drops below the lower threshold, an event is detected and depending on its duration and amplitude, is classified according to Table 1 [2].

Table 1. Classification of RMS events.

RMS Amplitude [pu]	Duration [s]	Type of event
< 0.1	< 3	Momentary interruption
	≥ 3 & < 60	Temporary interruption
	≥ 60	Sustained interruption
≥ 0.1 < 0.9	< 60	Sag
	≥ 60	Undervoltage
> 1.1	< 60	Swell
	≥ 60	Overvoltage

2.2. Detection of transients and waveform distortions

To detect transients and waveform distortions, the fundamental component of voltage u_1 must be separated from the other frequency components u_ε. This is achieved using four-parameter sine fitting which is used to determine the parameters of the fundamental [24]

$$u_{norm} = u_1 + u_\varepsilon. \tag{3}$$

The residuals u_ε, obtained after removing the fundamental component, contain the possible disturbances. These residuals can take both positive and negative values, and therefore, their absolute values are processed using the morphological closing operation [25] with a 50 ms structuring element (equivalent to 2.5 periods of the fundamental nominal frequency)

$$u_{closing} = |u_\varepsilon| \cdot s_{50}. \tag{4}$$

Morphological closing is used to eliminate the multiple crossings of the threshold that could belong to a single event [13]. The values obtained after the morphological closing are compared with a threshold to detect the events.

Depending on their duration, events are classified as transients or waveform distortions (Table 2). An event with duration below 20 ms will be identified as a transient and an event that has a duration above 50 ms will be identified as a waveform distortion. Separating the events with duration between 20 ms and 50 ms into transients or waveform distortions is done by thresholding the total harmonic distortion of the event. If the event's THD is below a threshold, then it is classified as a transient, otherwise as a waveform distortion.

Table 2. Classification of transients and waveform distortion.

Duration [s]	THD	Type of event
< 0.02	-	Transient
≥ 0.02 < 0.05	< THD_{THR}	Transient
	≥ THD_{THR}	Waveform distortion
≥ 0.05	-	Waveform distortion

The THD values are calculated using the amplitudes of the harmonics (up to the 50th) determined by applying the multiharmonic least-squares fitting algorithm [23]. According to the Fourier series, the signal can be decomposed in a sum of sine waves of frequencies $h \times f$, multiple of the fundamental frequency f, with amplitudes D_h and phases ϕ_h

$$
\begin{aligned}
y(t) &= C + \sum_{h=1}^{H_{total}} D_h \cos(2\pi hft + \phi_h) \\
&= C + \sum_{h=1}^{H_{total}} \left[A_h \cos\left(2\pi hft + \phi_h\right) + B_h \sin\left(2\pi hft + \phi_h\right) \right]
\end{aligned}
\tag{5}
$$

where H_{total} is the total number of harmonics that reconstruct the signal, C is the dc component, f is the fundamental frequency and A_h and B_h are the in-phase and in-quadrature amplitudes of harmonic h.

The multiharmonic fitting algorithm can estimate the amplitudes and phases only for the first H harmonics of the sampled signal. Considering that N samples $\mathbf{y} = [y_1 \ldots y_n \ldots y_N]^T$ are acquired at a f_s sampling rate, this algorithm estimates the values of A_h, B_h, C_h and f which minimize the sum of squared differences

$$
\sum_{n=1}^{N} \left[y_n - C - \sum_{h=1}^{H} \left[A_h \cos\left(2\pi hft_n + \phi_h\right) + B_h \sin\left(2\pi hft_n + \phi_h\right) \right] \right]^2 ,
\tag{6}
$$

where $t_n = (n-1)/f_s$ are the sample timestamps.

Either using the DFT, the inverse of the average time between three consecutive zero-crossings or other method for frequency measurement, an initial estimation of the fundamental frequency is made. This value is used to determine the initial harmonic parameters of the signal. A two-column matrix is built to calculate the harmonic parameters

$$
W_h = \left[\cos\left(2\pi hft\right) \quad \sin(2\pi hft) \right]
\tag{7}
$$

where $h = 1 \ldots H$ and $\boldsymbol{t} = \begin{bmatrix} t_1 & \ldots & t_n & \ldots & t_N \end{bmatrix}^T$.

For all the harmonics, the matrix used to determine C, A_h and B_h is

$$\boldsymbol{D} = \begin{bmatrix} \mathbf{1} & \boldsymbol{W}_1 & \ldots & \boldsymbol{W}_h & \ldots & \boldsymbol{W}_H \end{bmatrix}. \tag{8}$$

The least-squares solution vector

$$\boldsymbol{x_0} = \begin{bmatrix} C & A_1 & B_1 & \ldots & A_h & B_h & \ldots & A_H & B_H \end{bmatrix}^T \tag{9}$$

is determined by

$$\boldsymbol{x_0} = \left(\boldsymbol{D}^T \boldsymbol{D} \right)^{-1} \left(\boldsymbol{D}^T \boldsymbol{y} \right). \tag{10}$$

The determined parameters are calculated according to the value of the initial estimated fundamental frequency. To improve the frequency estimation, an iterative process is started where, at iteration i, all the parameters $A_h^{(i)}$, $B_h^{(i)}$ and $f^{(i)}$ are adjusted to minimize the least-squares error. The matrix used in the iterative process is

$$\boldsymbol{D}^{(i)} = \begin{bmatrix} \boldsymbol{Q} & \mathbf{1} & \boldsymbol{W}_I & \ldots & \boldsymbol{W}_h & \ldots & \boldsymbol{W}_H \end{bmatrix}, \tag{11}$$

where $\boldsymbol{Q}$ is a one-column matrix used for frequency correction

$$\boldsymbol{Q} = \sum_{h=1}^{H} \left[-A_h^{(i-1)} h \boldsymbol{t} \sin\left(2\pi h f^{(i-1)} \boldsymbol{t} \right) + B_h^{(i-1)} h \boldsymbol{t} \cos\left(2\pi h f^{(i-1)} \boldsymbol{t} \right) \right]. \tag{12}$$

At iteration i the estimated parameter vector is

$$\boldsymbol{x}^{(i)} = \begin{bmatrix} \Delta\omega^{(i)} & C^{(i)} & A_1^{(i)} & B_1^{(i)} & \ldots & A_h^{(i)} & B_h^{(i)} & \ldots & A_H^{(i)} & B_H^{(i)} \end{bmatrix}^T \tag{13}$$

and is obtained with

$$\boldsymbol{x}^{(i)} = \left[\left(\boldsymbol{D}^{(i)} \right)^T \boldsymbol{D}^{(i)} \right]^{-1} \left[\left(\boldsymbol{D}^i \right)^T \boldsymbol{y} \right]. \tag{14}$$

After each iteration, the frequency estimate is updated according to

$$f^{(i+1)} = f^{(i)} + \frac{\Delta\omega^{(i)}}{2\pi}. \tag{15}$$

Using the new values of $A_h^{(i)}$, $B_h^{(i)}$ and $f^{(i)}$ the iterative process continues until the absolute frequency changes are smaller than a threshold value.

In the iterative version of the multiharmonic fitting algorithm, the correction of frequency and harmonic parameters is done by introducing the element $\boldsymbol{Q}$ (see (12)) and an iterative process. In the non-iterative version of multiharmonic fitting algorithm the frequency is determined using the four-parameter sine fitting algorithm [24].

3. Improving the power quality detection algorithm

In order for the algorithm to be able to detect and classify events in real time, it must be able to perform all the waveform analysis within the time corresponding to the segment of data acquired. During the implementation of the algorithm, problems arose in terms of

reducing the time necessary to compute the multiharmonic least-squares fitting and choosing a suitable length of the data segment to be acquired.

To reduce the computing time of the multiharmonic algorithm three approaches were considered: (i) determine matrix (11) which will be then the subject of operations: transpose, multiplication and inversion which corresponds to step by step implementation of (14); (ii) calculate the pseudo-inverse of matrix (11) and multiplying the result with the signal matrix, because

$$\left[\left(\boldsymbol{D}^{(i)}\right)^T \boldsymbol{D}^{(i)}\right]^{-1} \left(\boldsymbol{D}^{(i)}\right)^T \boldsymbol{y} = \left[\boldsymbol{D}^{(i)}\right]^{\dagger} \boldsymbol{y} \tag{16}$$

where $\left[\boldsymbol{D}^{(i)}\right]^{\dagger}$ is the pseudoinverse of $\boldsymbol{D}^{(i)}$; (iii) directly calculating $\left(\boldsymbol{D}^{(i)}\right)^T \boldsymbol{D}^{(i)}$ and $\left(\boldsymbol{D}^{(i)}\right)^T \boldsymbol{y}$ after which the inversion and multiplication are applied. In this case, the fact is taken into account that the resulting matrix of $\left(\boldsymbol{D}^{(i)}\right)^T \boldsymbol{D}^{(i)}$ is symmetric below the main diagonal. This approach was improved by calculating only the elements on or above the main diagonal and the elements below the main diagonal were later copied from the elements above the main diagonal. The size of these two matrices does not depend on the number of processed samples.

The execution time of these three approaches for the iterative multiharmonic least-squares fitting (MHLSF) can be observed in Fig. 3 and for the non-iterative multiharmonic fitting in Fig. 4, in both cases as a function of the number of samples in each segment.

As it can be seen, the fastest approach is to calculate the matrix and after that applying the further operations step by step. Also, between the iterative and non-iterative algorithms the non-iterative one is, as expected, faster. This is because a smaller matrix is used in the process but mostly due to the number of iterations required in the iterative version of the algorithm.
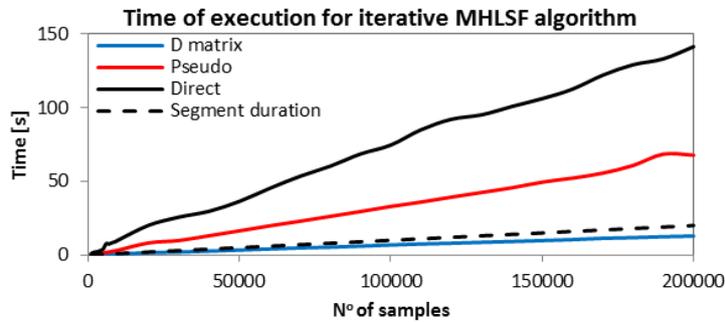

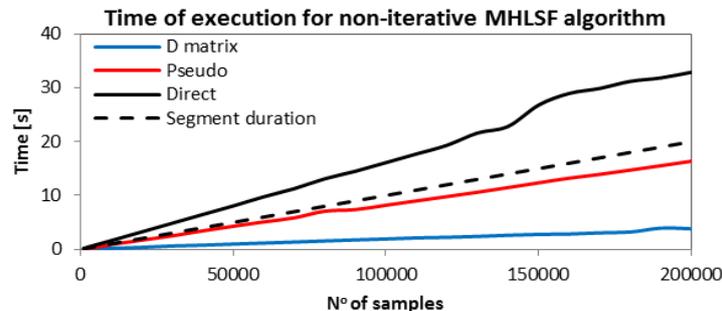Fig. 3. Execution time for iterative MHLSF algorithm.

Fig. 4. Execution time for non-iterative MHLSF algorithm.

The next step for improving the algorithm is to select an adequate length for the segment of data so the algorithm can perform all the analysis required to identify and classify, in real time, the power quality events. The system is set to acquire all the data available, but never less than the minimum segment length. The algorithm was tested for different values of the minimum segment length and the actual size of the acquired segment was registered while the algorithm performed its analysis for detecting power quality events (Fig. 5).
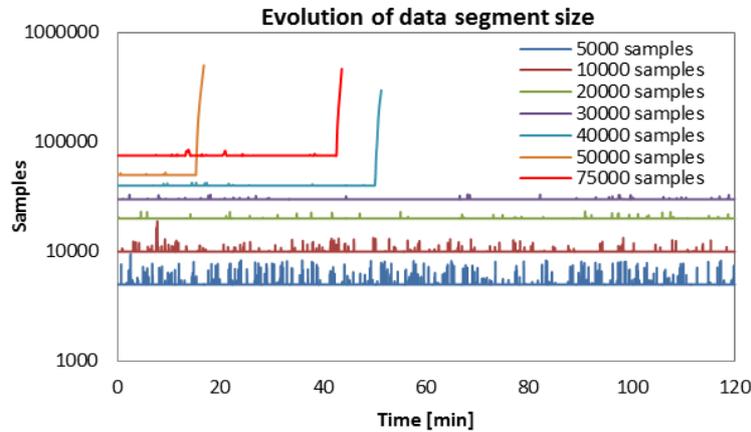

Fig. 5. Evolution of data segment size for 2 hours. The algorithm failed for 40 000, 50 000 and 75 000 samples per segment as can be seen from the sudden and irrecoverable increase in data segment size.

As can be seen in Fig. 5, for data segments larger than 30 000 samples (3 seconds of data), the size of the data segments remains approximately constant for a period of time, after which it begins to increase until the system fails. This increase corresponds to detection of an event whose processing is large enough to request such a computational effort from the algorithm, that it cannot keep up with the increased backlog of acquired data.

For segments of data smaller than 40 000 samples, increases in data segment sizes can be seen (they correspond to detection of events), but after a short time the size of data segments returns to the minimum value set. This means that, although the next segments were larger than the minimum defined size, the algorithm was able to process the additional samples in the next segments fast enough to recover the delay. Therefore, it can be said that the algorithm is stable for data segments whose size is below 40 000 samples. Taken into account these results, 20 000 samples (2 seconds of data) was chosen as the size of the data segment to be analyzed by the algorithm.

4. Measurement results

The system described in this paper is used to monitor the three phases of the power system to detect and classify the events that are occurring. Threshold u_{RMS+} was set at a value of 1.1 pu, u_{RMS-} at 0.9 pu, $clos_{THR}$ at 0.08 pu and THD_{THR} at 0.03.

In Fig. 6, a distortion of 121.7 ms duration and 0.114 pu maximum amplitude is shown. The values obtained from the morphological closing operation (Fig. 6A) are compared against the preset threshold value of 0.08 pu to find the start and end of the event. For this particular example the start is detected at t = 208.2 ms when the values rise to 0.09 pu from 0.079 pu and the end at t = 329.8 ms when the values fall from 0.08 pu to 0.739 pu. Considering this information, the time instants when the morphological closing values cross 0.08 pu are determined by interpolation and are then used to calculate the duration of the event. During this distortion the maximum amplitude of 0.114 pu is recorded at t = 279.2 ms. In Fig. 6B, the

zoom of the event start can be observed. Before the start, the waveform is beginning to distort but only after the starting point the distortion becomes more pronounced.
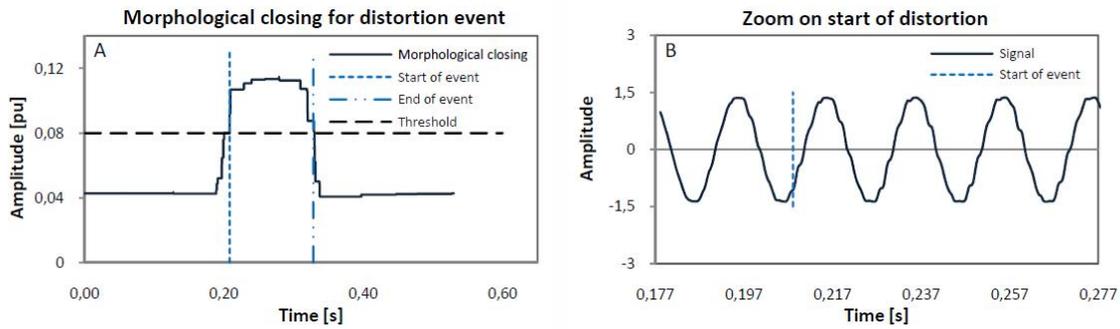

Fig. 6. Distortion event. A represents the result of the morphological closing operation applied to the signal's residuals with a structuring element of 50 ms and B is a zoom of the voltage waveform at the start of the distortion event.

In Fig. 7, a transient event of 1.73 ms duration and 0.478 pu amplitude can be observed. The value obtained with morphological closing (Fig. 7A) exceeds the threshold value from $t = 200$ ms (from 0.033 pu to 0.112 pu) until $t = 201.6$ ms (from 0.081 pu to 0.074 pu). The maximum amplitude is recorded at $t = 200.2$ ms. In Fig. 7B, the zoom of the transient event is shown where it can be observed, at the beginning of the event, the first spike that corresponds to the maximum value previously mentioned.
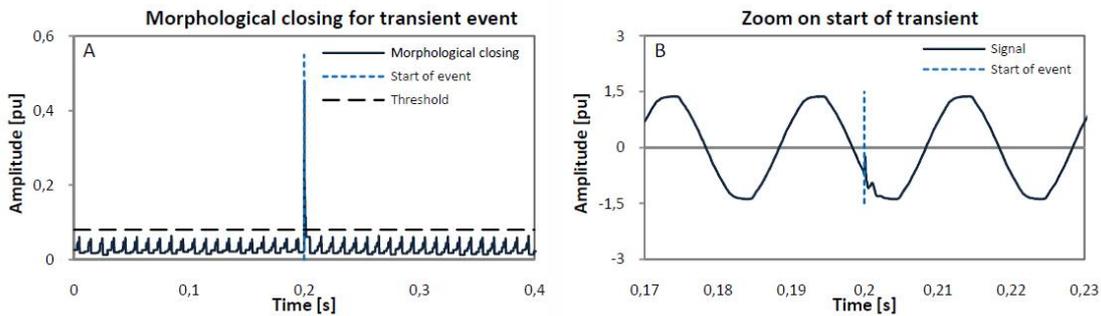

Fig. 7. Transient event. A represents the result of the morphological closing operation applied to the signal's residuals with a structuring element of 4 ms and B is a zoom of the voltage waveform at the start of the transient event.

In Fig. 8, a sag event of 211 ms duration is shown, during which the voltage amplitude dropped to a minimum of 0.75 pu. The correlation between the drop of the calculated RMS values (Fig. 8A) and a decrease of the amplitude of the voltage (Fig. 8B) can be observed. The event starts at $t = 210$ ms and ends at $t = 420$ ms, during that time the RMS values decrease to a minimum value of 0.75 pu near $t = 360$ ms.
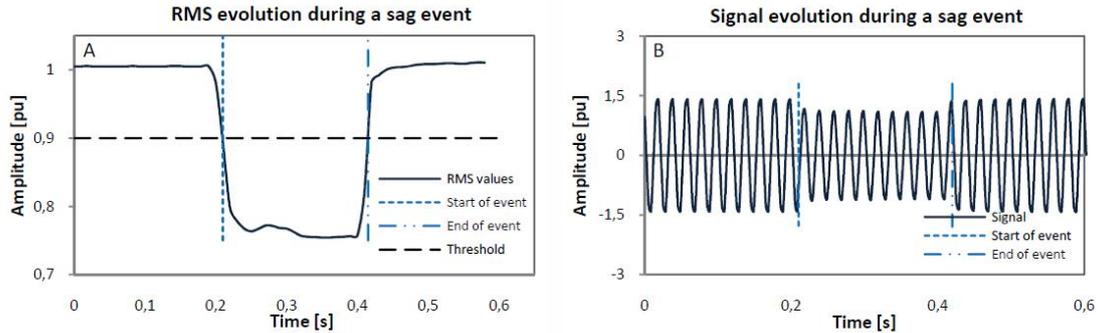
Fig. 8. Sag event. A is the evolution of the RMS values of voltage waveform during a sag event and B is the voltage waveform during a sag event.

An RMS event can occur anywhere in the acquired segment of data, meaning that the amplitude of the fundamental does not remain constant during that segment of data. Because the four-parameter sine fitting determines an average value of the fundamental component over the all segment of data, the residuals obtained after separating the fundamental component can cause the system to detect false transients or waveform distortions (Fig. 9). For segments of data without events, the amplitudes of the closing signal have values below 0.08 pu. However, in the example given in Fig. 9, because of the RMS event, those values are much higher and the algorithm will detect a waveform distortion which does not exist. Because of this, whenever a transient or waveform distortion is detected during a RMS event, a warning message will be recorded into the file that contains the information about the respective event (waveform distortion or transient) indicating the occurrence of a RMS event during the same time period.
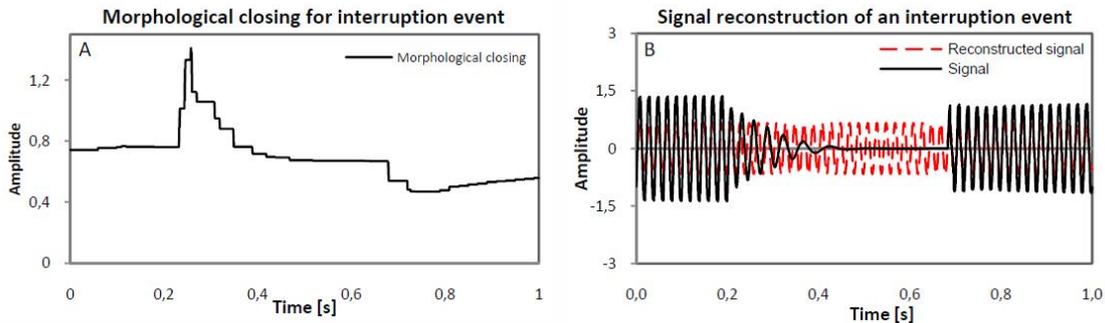

Fig. 9. Signal's reconstruction and closing signal at a RMS event. A represents the result of the morphological closing operation applied to the signal's residuals with a structuring element of 50 ms and B is the original and reconstructed signal.

5. Conclusions

In this paper, the implementation of an improved algorithm for power quality monitoring is presented. RMS events are detected by analyzing the RMS values of the voltage calculated at a rate of a half of period for one period of the signal in accordance with IEC 61000-4-30 [3]. Interpolation was used to find the zero crossings of the signal which improved the accuracy of the determined RMS values. For transient and waveform distortion detection, the fundamental component was separated from the normalized voltage signal, thus obtaining a residual signal which was used for event detection. The absolute values of the residuals were processed using morphological closing to facilitate event detection. Detected events whose durations were less than 20 ms were classified as transients and the ones whose duration was more than 50 ms

were identified as waveform distortions. Between these limits, the separation between transients and waveform distortions was made using the THD values. In order to calculate THD values, the multiharmonic least-squares fitting algorithm was used. As this was the algorithm with higher computational requirements, three different proposed implementations were compared to select the fastest implementation. Also, between the iterative and non-iterative implementation of the multiharmonic algorithm, the non-iterative one was found to be the quickest, because of the smaller matrix used and because it is non-iterative.

Next, the ideal length of data segment had to be found for which the algorithm could perform all the analysis needed for event detection in real time. For this, the algorithm was tested for different minimum sizes of data segments, from which the value that ensured proper operation was selected.

In the end, an algorithm for monitoring, detection and classification of power quality events in real time was successfully implemented. The system is fully operational for real time monitoring and the detected events are uploaded to a web server and are available at http://gim.lx.it.pt/fct57708/events/.

References

[1]   Targosz, R., Manson, J. (2007). Pan European LPQI Power Quality Survey. In *Proceedings of the 9th International Conference on Electric Power Quality and Utilisation 2007*, Barcelona, Spain.

[2]   IEEE Std 1159-1995. (1995). *IEEE Recommended Practice for Monitoring Electric Power Quality*. The Institute of Electrical and Electronics Engineers, Inc., New York, USA.

[3]   IEC 61000-4-30:2003. (2003). *Electromagnetic compatibility (EMC) – Part 4-30: Testing and measurement techniques – Power quality measurement methods*. International Electrotechnical Commission, Geneva, Switzerland.

[4]   Bollen, M.H.J., Gu, I.Y.H. (2006). *Signal Processing of Power Quality Disturbances*, John Wiley & Sons.

[5]   Santoso, S., Powers, E.J., Grady, W.M., Hofmann, P. (1996). Power quality assessment via wavelet transform analysis. *IEEE Transactions on Power Delivery*, 11(2), 924-930.

[6]   Gaouda, A.M., Salama, M.M.A., Sultan, M.R., Chikhani, A.Y. (1999). Power quality detection and classification using wavelet-multiresolution signal decomposition. *IEEE Transactions on Power Delivery*, 14(4), 1469-1476.

[7]   Poisson, O., Rioual, P., Meunier, M. (2000). Detection and measurement of power quality disturbances using wavelet transform. *IEEE Transactions on Power Delivery*, 15(3), 1039-1044.

[8]   Karimi, M., Mokhtari, H., Iravani M.R. (2000). Wavelet based on-line disturbance detection for power quality application. *IEEE Transactions on Power Delivery*, 15(4), 1212-1220.

[9]   He, H., Starzyk, J.A. (2006). A self-organizing learning array system for power quality classification based on wavelet transform. *IEEE Transactions on Power Delivery*, 21(1), 286-295.

[10] Kaewarsa, S., Attakitmongcol, K., Kulworawanichpong, T. (2008). Recognition of power quality events by using multiwavelet-based neural networks. *International Journal of Electrical Power & Energy Systems*, 30(4), 254-260.

[11] Uyar, M., Yildirim, S., Gencoglu, M.T. (2008). An effective wavelet-based feature extraction method for classification of power quality disturbance signals. *Electric Power Systems Research*, 78(10), 1747-1755.

[12] Artioli, M., Pasini, G., Peretto, L., Sasdelli, R., Filippetti, F. (2004). Low-cost DSP-based equipment for the real-time detection of transients in power systems. *IEEE Transactions on Instrumentation and Measurement*, 53(4), 933-939.

[13] Radil, T., Ramos, P.M., Janeiro, F.M., Serra, A.C. (2007). DSP Based Power Quality Analyzer for Detection and Classification of Disturbances in a Single-phase Power System. *Metrology and Measurement Systems*, 14(4), 483-494.

[14] Mindykowski, J., Tarasiuk, T. (2010). Development of DSP-based instrumentation for power quality monitoring on ships. *Measurement*, 43(8), 1012-1020.

[15] Radil, T., Ramos, P.M., Janeiro, F.M., Serra, A.C. (2008). PQ Monitoring System for Real-Time Detection and Classification of Disturbances in a Single-Phase Power System. *IEEE Transactions on Instrumentation and Measurement*, 57(8), 1725-1733.

[16] Radil, T., Janeiro, F.M., Ramos, P.M., Serra, A.C. (2008). An efficient approach to detect and classify power quality disturbances. *COMPEL – The International Journal for Computation and Mathematics in Electrical and Electronic Engineering*, 27(5), 1178-1191.

[17] Perez, E., Barros, J. (2008). A proposal for on-line detection and classification of voltage events in power systems. *IEEE Transactions on Power Delivery,* 23(4), 2132-2138.

[18] Zhu, F.-F., Hu, G.-S., Xie, J. (2005). Classification of power quality disturbances using wavelet and fuzzy support vector machines. *Proceedings of the 4th International Conference on Machine Learning and Cybernetics*, (7), 3981-3984.

[19] Gaing, Z.-L. (2004). Wavelet-based neural network for power quality disturbance recognition and classification. *IEEE Transactions on Power Delivery*, 19(4), 1560-1568.

[20] Gaouda, A.M., Kanoun, S.H., Salama, M.M.A., Chikhani, A.Y. (2002). Pattern Recognition Applications for Power System Disturbance Classification. *IEEE Transactions on Power Delivery,* 17(3), 677-683.

[21] Wang, M., Rowe, G.I., Manishev, A.V. (2004). Classification of power quality events using optimal time-frequency representations, theory and application. *IEEE Transactions on Power Delivery*, 19(3), 1496-1503.

[22] Chen, Z., Urwin, P. (2001). Power Quality Detection and Classification Using Digital Filters. *2001 IEEE Porto Power Tech Proceedings*, (1), 6.

[23] Ramos, P.M., Silva, M.F., Martins, R.C., Serra, A.M.C. (2006). Simulation and experimental results of multiharmonic least-squares fitting algorithms applied to periodic signals. *IEEE Transactions on Instrumentation and Measurement*, 55(2), 646-651.

[24] IEEE Std 1057-2007 (2008). *IEEE Standard for Digitizing Waveform Recorders*, The Institute of Electrical and Electronics Engineers, Inc., New York, USA.

[25] Serra, J. (1982). Image analysis and mathematical morphology. *Academic Press*, Inc.